Spectral characterization of integrated acousto-optic tunable filters by means of laser frequency modulation spectroscopy

Antonio Di Maio, Mario Salza, Gianluca Gagliardi, Pietro Ferraro, and Paolo De Natale

The spectral characteristics of an integrated acousto-optic tunable filter (AOTF) as well as its responsivity to the rf driving signal and sensitivity to temperature changes are experimentally investigated and quantified using a diode-laser-based interrogation system. A spectroscopic technique, exploiting the rf frequency modulation of the laser beam and the phase-sensitive detection of the AOTF transmission, has been used for this purpose. That allows for the generation of a dispersivelike signal, which serves as a reference for tracking any wavelength change of the filter's peak with high resolution. The possibility of using the integrated AOTF as a spectrum analyzer with this interrogation scheme for fiber Bragg grating (FBG) strain sensing is also discussed.

OCIS codes: 230.1040, 140.2020, 060.2630.

1. Introduction

Since their first reported realization,[1] acousto-optic tunable filters (AOTFs) have found a wide range of applications: as a wavelength-selective optical filter (WDM switch–router or add–drop multiplexing) in densely packed multiwavelength optical networks,[2] as an Er-doped fiber-amplifier gain flattening, and as a tuning laser device.[3] In particular, AOTFs were used in the area of optical imaging[4] as well as biomedical and mechanical sensing.[5,6] Within this field, the capability to detect the static and dynamic shift of the fiber Bragg grating (FBG) peak wavelength has also been shown, using different optical schemes.[7–10]

To the best of our knowledge, there is still a lack of works reporting direct, high-resolution spectral characterization of AOTFs, besides a few based on optical spectrum analyzers (OSAs) in conjunction with broadband light sources, such as superluminescent LEDs, amplified-spontaneous emitters, and white-light point sources,[11–13] or in direct comparison between different realization designs and modeling.[14,15] OSAs' typical wavelength resolution, ranging from 0.1 to 0.05 nm, as well as their low scanning speed and sensitivity, may represent a limitation for the accurate reconstruction of the AOTF transmission spectrum. Furthermore, considerable interest has recently been directed to bandwidth analysis and the reduction of the filter's asymmetries relevant to the WDM optical communication systems.[13] A complete investigation of an FBG-based strain detection setup, relying on frequency-shift-keyed tracking of an AOTF, was carried out in Ref. 11, using a linear model to describe its behavior and estimate the resolution limit. The authors point out limitations coming from reproducibility limits and temperature stability of an AOTF device. On the other hand, most previous works were still focused on the performance test of conventional nonintegrated acousto-optic filters. This issue was partially addressed in Ref. 16, where the authors report on the use of a narrowband laser source to provide information on the spectral-purity features of an integrated AOTF, while only a preliminary estimate of filter response was performed. All these aspects may be of some interest in a number of applications, and particularly in those cases where the analyzer is employed for the high-sensitivity interrogation of the FBG sensors for strain measurements, the strain resolution being strictly related to the minimum detectable AOTF shift. In fact, though the use of conventional broadband radiation with AOTF devices presents noticeable advantages in terms of dynamic range and is well suited for multiple-sensor

The authors are with the CNR-Istituto Nazionale di Ottica Applicata and European Laboratory for Non-Linear Spectroscopy, Comprensorio "A. Olivetti," Via Campi Flegrei 34, 80078 Pozzuoli, Naples, Italy. G. Gagliardi's e-mail address is gagliardi@inoa.it.

Received 21 February 2006; revised 24 July 2006; accepted 23 August 2006; posted 28 August 2006 (Doc. ID 68282).

0003-6935/06/369176-06$15.00/0

schemes,[7] it is still possible to combine it with complementary setups, aimed at improving the resolution for small-strain sensing applications. In addition, characterization of the filter responsivity and its dependence on environmental parameters can improve the accuracy in calibration of bulk and integrated AOTF-based spectrometers.

Here, we propose a radically different method, which inherits all advantages of frequency-modulation (FM) spectroscopy, a well-established technique capable of rapidly and sensitively detecting narrow spectral features.[17,18] The high resolution achievable with a near-IR distributed-feedback (DFB) diode laser, combined with rf frequency-modulation spectroscopy, enables us to detect small and fast central-wavelength changes of an integrated AOTF as well as to extract information on the transmission spectral profile as a function of the operational conditions. Also, the signal resulting from the detection process can be adopted as a reference in active locking systems of the AOTF peak.

2. Experimental Approach

Our experimental scheme is depicted in Fig. 1. A current and temperature-controlled DFB diode laser (Sensors Unlimited SUI1393CFIFC), emitting ~1391 nm, with a linewidth of 10 MHz, delivers ~120 μW to a polarization-dependent integrated AOTF (Alenia IOS 17/11 P-T), through a polarization rotator and a polarization maintaining fiber. The integrated AOTF, fabricated in $LiNbO_3$, exploits collinear interaction between the guided optical radiation and a surface acoustic wave (SAW). The filter can be tuned by the SAW frequency and has a nominal bandwidth (FWHM) of ~0.45 nm. The acousto-optic crystal is temperature stabilized, within 0.002 °C, by means of a proportional-integral-derivative module (TED200) acting on an internal Peltier cooler, and its temperature is measured by a negative-temperature-coefficient sensor. The device central wavelength is driven by a rf signal, generated by a voltage-controlled oscillator (VCO), with an efficiency higher than 90% with an 8 mW power. The oscillator frequency is accurately and continuously monitored by a wide-bandwidth spectrum analyzer (Anristu MS2665C). A 1 GHz bandwidth p-i-n photodiode is used to detect the optical transmission of the AOTF to observe its sinc-shaped spectral response, as shown in Fig. 4 below.

Owing to the limited current tunability of the laser (0.13 nm), we usually keep the laser fixed while fast sweeping the AOTF center by summing a linear voltage scan to the VCO-frequency control input, V_t. In this way, we observe the AOTF spectral response at approximately the laser emission wavelength. Spectra recording and filter operational conditions are based on a preliminary measurement. Using an OSA (ANDO AQ6317B) and a broadband light source, we measured the AOTF responsivity, found to be approximately 4 nm/MHz, and its peak wavelength, which was ~1391.5 nm when driven by a 197.7 MHz signal. Hence since the AOTF bandwidth is 0.45 nm, we usually fix a spectral window of 1.5 nm, corresponding to a 300 kHz sweep.

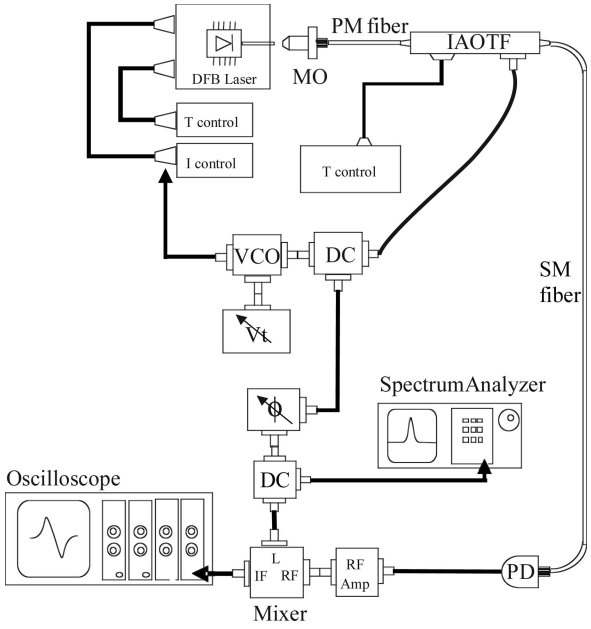

Fig. 1. Sketch of the experimental setup. DFB, distributed feedback; MO, microscope objective; DC, directional coupler; VCO, voltage-controlled oscillator; PD, photodiode; and IAOTF, integrated AOTF.

The high-sensitivity interrogation of the filter relies on heterodyne detection of the AOTF transmitted radiation when the laser source is nearly resonant with it. A FM at approximately $f = 200$ MHz is applied to the laser via the injection current, using the same rf signal sent to the acousto-optic filter. This generates a pair of sidebands with opposite phases at a distance f from the carrier frequency with a power ratio of a few percent. Since the typical tuning range used for the filter is of the order of 200–300 kHz, i.e., within the laser emission linewidth, the sweep of the VCO frequency does not cause any appreciable effect to the sidebands. The use of a distinct oscillator for laser FM should be considered only for wider AOTF frequency spans. The rf wave is partially routed by a directional coupler (DC) to a voltage-tunable phase shifter and then to the local oscillator (LO) of a double-balanced mixer (DBM). Demodulation at f of the amplified photodiode-output voltage is performed by the DBM, where optimal phase-sensitive detection is accomplished by adjusting the LO phase. The DBM intermediate frequency (IF) output produces a dc voltage proportional to the sum of the beat signals (f) between the two sidebands and the carrier, which is low-pass filtered at 5 kHz and displayed on a digital oscilloscope for acquisition and analysis. The variable phase delay allows for the selection of different components from the mixer signal: one directly dependent on the sidebands amplitude imbalance, also containing the residual laser amplitude modulation, and another basically derived from the differential sidebands dispersion, with a phase retardation of 90° with respect to the first term.[17] Therefore the IF out-

put is very sensitive to differences in phase and power experienced by the sidebands when they interact with the filter around its resonance. Choosing a proper phase shift between laser modulation and LO, the IF signal can be detected free of any additional DC offset due to the residual laser amplitude modulation contribution. Moreover, phase-sensitive selection also enables rejection of the possible spurious signals derived from power diffracted inside the acousto-optic modulator. When the laser wavelength is close to the AOTF center, and V_t is swept by a slow triangular wave, the DBM yields a symmetric, dispersivelike signal with a zero-crossing point located exactly at the filter-center wavelength. As a consequence, any change of the driving frequency or crystal temperature would result in detuning the AOTF curve with respect to the laser frequency, which is always maintained as stable. Hence such a system acts as a monitor of the integrated AOTF response to frequency variations of the driving signal as well as to environmental conditions, since these parameters directly affect the DBM signal amplitude. The corresponding voltage change can readily be detected in a small region around the center of the dispersive signal, where the amplitude-frequency dependence is linear. With a wavelength calibration of the spectrum, this voltage already contains the desired information on the frequency detuning applied to the AOTF. Using a laser as a radiation source increases the amount of available optical power, thus improving the sensitivity, while keeping the interrogation time very short. An additional advantage is derived from rf modulation and detection, which strongly reduces the amplitude excess noise due to the laser source and electronics,[18] while no complicated fitting procedure is necessary to extract the AOTF peak position, since it can be directly measured from the zero-crossing point of the acquired spectrum. Furthermore, compared to other passive techniques, the signal produced by the detection system has a zero background around the peak, and it is thus intrinsically more sensitive to wavelength shifts, which are converted by sideband dispersion into a voltage variation.

3. Results and Discussion

To characterize the responsivity and the sensitivity limits of our integrated AOTF device, we performed a set of repeated acquisitions of the phase-detected dispersive signals, each acquisition corresponding to a different V_t DC voltage that determines the VCO center frequency (and thus the AOTF center wavelength). Changes in the center position were chosen, which were very small in order to observe the behavior of the system for the fine tuning of the filter. Each of them was taken as the statistical mean of five VCO frequency readings of the spectrum analyzer.

At the same time, the VCO frequency span, over which the AOTF spectrum was observed, was calibrated in terms of laser wavelength. The relationship between the driving rf and the wavelength was retrieved in a subsequent measurement where the VCO was continuously swept around a fixed frequency center, while the laser temperature T_L was step varied along the whole span. This was possible because of the laser-wavelength temperature tunability that is of the order of 0.1 nm/°C. Hence for each selected T_L value, the laser wavelength was measured by a commercial wavemeter with a 10^{-7} accuracy (Burleigh model WA-1500), and served as a ruler for the conversion of the horizontal axis in nanometer units. In this way, we could determine the signal line shape and position in terms of the wavelength for different AOTF-signal frequencies with sufficient resolution and reliability.

In Fig. 2, an example of AOTF detection is shown for five different values of the VCO frequency, expressed on the axis as the laser wavelength, when it is swept at ~50 Hz. In Fig. 3, the center's positions are plotted versus the applied rf steps. It can be noted that the filter response exhibits a fairly linear behavior with a least-squares fit slope of 3.59 ± 0.02 nm/MHz. The AOTF crystal temperature was always maintained as stable during the measurement time by the Peltier module so that no thermal effect could cause systematic deviations in our measurements to better than 10^{-3} nm (maximum false shift for a temperature deviation of 0.002 °C), because of the stabilizing-loop efficiency and the low power necessary to drive the acoustic transducer. On the other hand, the short-term stability is expected to be even better, mostly depending on the oscillator frequency jitter. Analogous considerations can be done for the laser wavelength stability, for which only a maximum drift of 10^{-3} nm can be present over a measurement time exceeding 1 h.

As a further investigation, the same step measurements were repeated considering a possible temperature dependence of the AOTF response. Indeed, the sinc^2 transmission function of the device is centered at the wavelength $\lambda_p = V_{ac}(n_{\mathrm{TM}} - n_{\mathrm{TE}})/f$ determined by the speed V_{ac} and the frequency f of

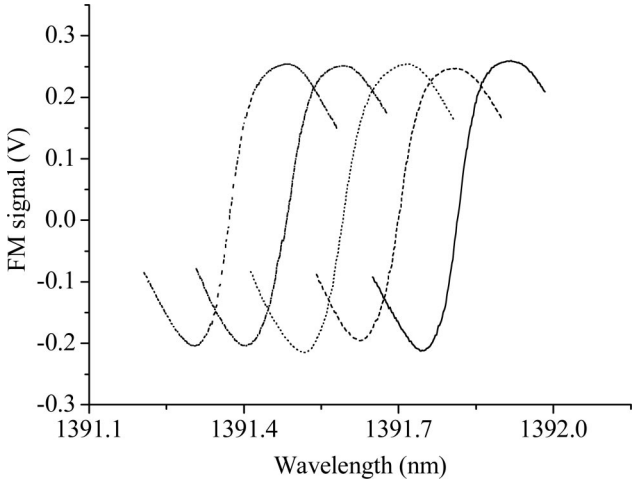

Fig. 2. AOTF curves, observed by the FM technique, for different tuning frequencies (T_{AOTF} = 23.948 °C). The signals were noise filtered within a detection bandwidth of 5 kHz.

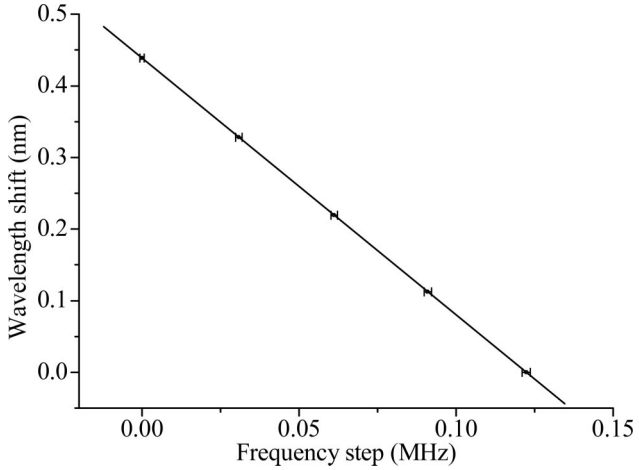

Fig. 3. Shift resulting from Fig. 2 has an almost perfect linear dependence on the rf frequency step (3.59 ± 0.02 nm/MHz). The uncertainty in the center determination is represented by the horizontal bars.

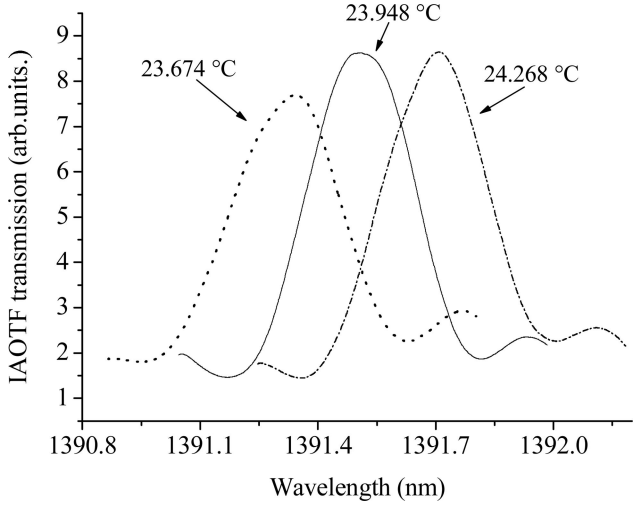

Fig. 4. AOTF transmission spectrum at three different temperatures. A large shift of the center as well as a change in the line shape is clearly visible between the curves.

the SAW and by the refractive indexes n_{TM} and n_{TE} of the guided polarization modes TM and TE. The crystal birefringence as well as the sound propagation speed are dependent on the temperature. Therefore we acquired both the directly transmitted and the heterodyne-detected AOTF spectra scanning the VCO frequency around a fixed center, at different Peltier-controlled temperatures. Figure 4 shows the direct-transmission line shape of the AOTF for T_{AOTF} = 23.674 °C, 23.948 °C, and 24.268 °C. Here, a slight asymmetry in the spectral profile manifests for increasing temperature, with a pronounced sidelobe at longer wavelengths,[19] as well as a temperature-induced shift. From the zero-crossing positions of dispersive signals acquired at the selected temperatures, we measured the wavelength shifts and obtained the data shown in Fig. 5. A linear fit yielded a temperature tuning factor of (0.616 ± 0.004) nm/°C, in agreement with a preliminary measurement by an OSA. Subsequently, to investigate possible effects of thermal variations on the filter's tuning sensitivity, the spectra corresponding to another group of temperature values were recorded when the filter's driving frequency was step varied by a small amount and symmetrically scanned along 200 kHz. The zero crossings versus the VCO center gave linear slopes very close to each other for all temperature values, as shown in Fig. 6. In particular, we found the factors −3.73 ± 0.01, −3.62 ± 0.03, −3.65 ± 0.02, −3.63 ± 0.02 nm/MHz for T_{AOTF} = 23.820 °C, 23.674 °C, 24.103 °C, and 24.268 °C, respectively. The experimental slopes were randomly distributed around the mean value of 3.66 nm/MHz and were all consistent within 3σ. This result confirms, at least in this range, that temperature does not significantly affect the AOTF responsivity.

Since both the laser and the filter were kept at a stable temperature, the fluctuations on the responsivity factors likely include noise and instability sources related to the oscillator. From the mean value found above, given a rms VCO frequency ripple of ~3 kHz, the reproducibility performance of our diagnosis system is effectively limited to a minimum detectable wavelength shift of approximately 10 pm due to the oscillator quality. This is in good agreement with the standard deviation found for the AOTF rf-tuning slope (0.02 nm). Using a higher-stability oscillator, even smaller AOTF's center shifts could be detected directly from the DC mixer output changes, expressed in terms of laser wavelength. It is worth noting that our measurement procedure was extremely fast as the duration of each VCO sweep was 10 ms. No long-time averaging was applied to the AOTF signals for noise reduction, which was collected in an effective bandwidth of 5 kHz. This aspect must also be taken into account when comparing the minimum wavelength resolution of our system to others.

In the case where the integrated AOTF is used as a spectrum analyzer for FBG sensor interrogation,

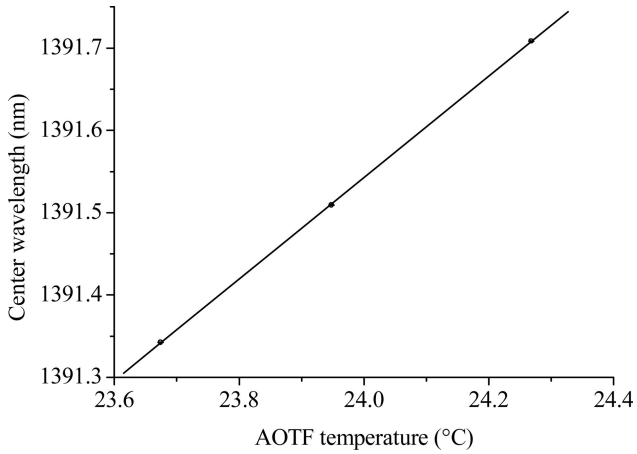

Fig. 5. Linear shift of the AOTF center wavelength measured by phase-sensitive demodulation of the transmitted power for temperatures 23.674 °C, 23.948 °C, and 24.268 °C. The slope value is (0.616 ± 0.004) nm/°C.

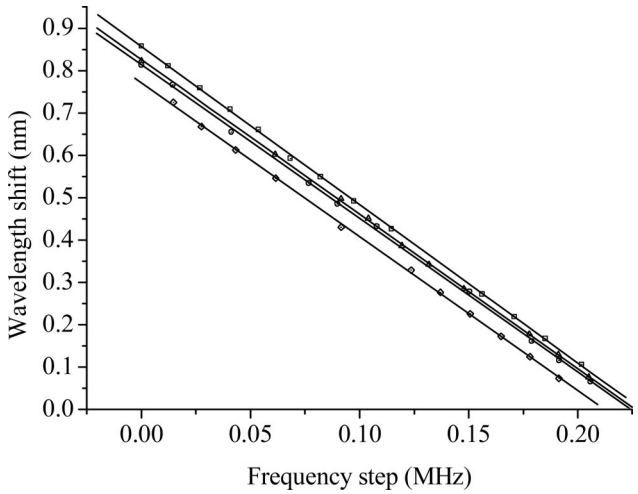

Fig. 6. Linear tuning response of the AOTF at four different Peltier-controlled temperatures: 23.820 °C (square symbols), 23.674 °C (circles), 24.103 °C (triangles), 24.268 °C (rhombuses). The slope values are all in good agreement within three standard deviations. The wavelength shift uncertainty is contained in the point size.

our approach can be suitable for this purpose. Indeed, the AOTF can be probed by a fiber-coupled sideband-modulated diode laser while it detects the FBG transmitted or reflected beam. The phase-sensitive-detected dispersive signal from the AOTF could thus be used to steer an active frequency-locking system that makes the AOTF track the Bragg sensor's movements due to mechanical or thermal actions. In this way, the strain information can be extracted from the acousto-optic filter when the laser keeps the filter's center locked to the Bragg resonance. The locking-loop error signal fed back to the oscillator serves as a monitor, and the strain value can be readily retrieved from the oscillator frequency, once the filter response is known. The setup can be conveniently adopted to replace frequency-shifted-key schemes and to exploit laser spectral resolution while keeping the advantage of a high-dynamic-range sensing approach because of the combination of a widely tunable filter.

4. Conclusions

We have proposed and demonstrated a novel method capable of rapidly and sensitively detecting the narrow spectral features of a tunable filter, combining a laser source and a frequency-modulation spectroscopic technique. Reported results show that this scheme enables high-resolution spectral reconstruction of the response function of acousto-optic filters. Particularly, measurements on our integrated AOTF show a responsivity factor of the order of 3.7 nm/MHz, in good agreement with those expected from the manufacturer's data. Using the same approach, we investigated thermal effects on the AOTF response and measured the temperature tuning factor. Also, we checked that the responsivity values still hold true for small temperature variations of the internal acousto-optic crystal. The present sensitivity limit, as a minimum detectable wavelength shift, is 10 pm. Most limitations can be addressed to the frequency instability of the rf oscillator. Use of a phase-locked loop oscillator or an autoreferenced synthesized source can dramatically improve the performance of our system, thus pointing out the actual resolution of the method for AOTF filter interrogation. The procedure we implemented can be extremely useful in view of testing and calibrating different acousto-optic filters used as spectrum analyzers in FBG-based strain-measurement apparatuses and can be complementary to broadband, conventional techniques. These filters, indeed, may be responsible for resolution limitation in the interrogation process. Furthermore, the method has the potentiality to accurately measure variations of several different parameters, such as AOTF linewidth and peak wavelength, as a consequence of thermal effects.[19] This may be relevant for all kinds of optical tunable filters exhibiting a narrow bandwidth.

The authors thank Alenia Aeronautica for having supplied part of the optical equipment necessary for the experiment.

References

1. J. Frangen, H. Herrmann, R. Ricken, H. Seibert, W. Sohler, and E. Strake, "Integrated optical, acoustically tunable wavelength filter," in Proc. SPIE **1141,** 149–153 (1989).
2. D. A. Smith, J. E. Baran, J. J. Johnson, and K.-W. Cheung, "Integrated-optic acoustically-tunable filters for WDM networks," IEEE J. Sel. Areas Commun. **8,** 1151–1159 (1990).
3. D. A. Smith and Z. Bao, "Technology and applications of the integrated acousto-optic filter," in *Proceedings of the Eighth Mediterranean Electrotechnical Conference on Industrial Applications in Power Systems, Computer Science and Telecommunications* (MELECON 96) (IEEE, 1996), pp. 100–107.
4. N. Gupta, D. R. Suhre, and M. Gottlieb, "Long-wave infrared imager with an 8-cm^{-1} passband acousto-optic tunable filter," Opt. Eng. **44,** 094601 (2005).
5. N. Gupta, "Acousto-optic-tunable-filter-based spectropolarimetric imagers for medical diagnostic applications-instrument design point of view," J. Biomed. Opt. **10,** 051802 (2005).
6. X. Wang, D. E. Vaughan, V. Pelekhaty, and J. Crisp, "A novel miniature spectrometer using an integrated acousto-optic tunable filter," Rev. Sci. Instrum. **65,** 3653–3656 (1994).
7. M. Volanthen, H. Geiger, M. G. Xu, and J. P. Dakin, "Simultaneous monitoring fibre gratings with a single acousto-optic tunable filter," Electron. Lett. **32,** 1228–1229 (1996).
8. H. Geiger, M. G. Xu, N. C. Eaton, and J. P. Dakin, "Electronic tracking system for multiplexed fibre grating sensors," Electron. Lett. **32,** 1006–1007 (1995).
9. M. G. Xu, H. Geiger, J. L. Archambault, L. Reeckie, and J. P. Dakin, "Novel interrogating system for fibre Bragg grating sensors using an acousto-optic tunable filter," Electron. Lett. **29,** 1510–1511 (1993).
10. J. R. Dunphy, P. Ferraro, S. Inserra Imparato, G. Meltz, M. Signorazzi, A. Vannucci, M. Varasi, and C. Voto, "Integrated optical instrumentation for the diagnostics of parts by embedded or surface attached optical sensors," U.S. patent 5,493,390 (20 February 1996).
11. M. G. Xu, H. Geiger, and J. P. Dakin, "Modeling and performance analysis of a fiber Bragg grating interrogation system using an acousto-optic tunable filter," J. Lightwave Technol. **14,** 391–396 (1996).
12. A. Y. S. Cheng, J. Zhu, and M. C. Y. Pau, "Characterization of a noncollinear acousto-optic tunable filter and its resolution

enhancement as a near-infrared spectrometer," Appl. Spectrosc. **55,** 350–355 (2001).
13. D. R. Suhre and N. Gupta, "Acousto-optic tunable filter sidelobe analysis and reduction with telecentric confocal optics," Appl. Opt. **44,** 5797–5801 (2005).
14. C. D. Tron and G. C. Huang, "Characterization of the collinear beam acousto-tunable filter and its comparison with the noncollinear and the integrated acousto-optic tunable filter," Opt. Eng. **38,** 1143–1148 (1999).
15. H. Mendis, A. Mitchell, I. Belski, M. Austin, and O. A. Peverini, "Design, realisation and analysis of an apodised, film-loaded acousto-optic tunable filter," Appl. Phys. B **73,** 489–493 (2001).
16. M. Varasi, M. Signorazzi, A. Vannucci, and J. Dunphy, "A high-resolution integrated optical spectrometer with applications to fibre sensor signal processing," Meas. Sci. Technol. **7,** 173–178 (1996).
17. G. C. Bjorklund, M. D. Levenson, W. Lenth, and C. Ortiz, "Frequency modulation (FM) spectroscopy," Appl. Phys. B **32,** 145–152 (1983).
18. J. A. Silver, "Frequency-modulation spectroscopy for trace species detection: theory and comparison among experimental methods," Appl. Opt. **31,** 707–717 (1992), and references therein.
19. D. A. Smith, A. D'Alessandro, H. Herrmann, and J. E. Baran, "Source of sidelobe asymmetry in integrated acousto-optic filters," Appl. Phys. Lett. **62,** 814–816 (1993).